ACS APPLIED MATERIALS & INTERFACES

Letter

www.acsami.org

Synthesis and Nonvolatile Memory Behaviors of Dioxatetraazapentacene Derivatives

Gang Li,[†] Ke Zheng,[‡] Chengyuan Wang,[†] Kheng Swee Leck,[‡] Fangzhong Hu,*[,§] Xiao Wei Sun,*[,‡,⊥] and Qichun Zhang*[,†]

[†]School of Materials Science and Engineering, Nanyang Technological University, Singapore 639798

[‡]School of Electrical and Electronics Engineering, Nanyang Technological University, Singapore 637371

[§]State Key Laboratory and Institute of Elemental-Organic Chemistry, Nankai University, Tianjin, P. R. China 300071

[⊥]South University of Science and Technology, 1088 Xue-Yuan Road, Shenzhen, Guangdong, China 518055

Supporting Information

ABSTRACT: Two novel heteroacenes 2,3,9,10-tetra(furan-2-yl)-1,4,8,11-tetraaza-6,13-dioxapentacene (**FAOP**, **1**) and 2,3,9,10-tetra(thiophen-2-yl)-1,4,8,11-tetraaza-6,13-dioxapentacene (**TAOP**, **2**) was successfully synthesized through a one-step condensation reaction, which have been fully characterized by ^{1}H NMR (nuclear magnetic resonance), ^{13}C NMR, FT-IR (Fourier transform infrared spectroscopy), and HRMS (high-resolution mass spectrum). The sandwich-structure memory devices have been fabricated using **FAOP** (**1**) and **TAOP** (**2**) as active layers, showing a typical bipolar resistive switching (RS) behavior in positive and negative regions.

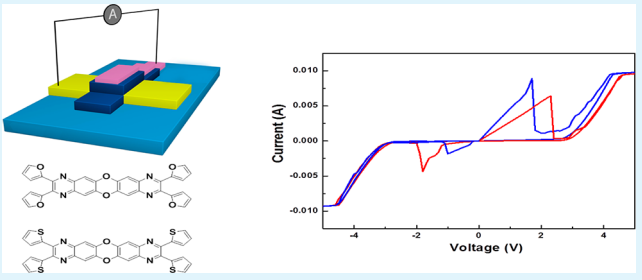

KEYWORDS: *synthesis, nonvolatile memory, condensation reaction, heteroacenes, bipolar resistive switching*

1. INTRODUCTION

Introducing heteroatoms into the backbone of conjugated oligoacene systems[1−10] will offer us more opportunities to tune their properties because HOMO−LUMO gap, HOMO/LUMO positions, and stability strongly depends on the types (e.g., N, O, P, B), the position, and the number of heteroatoms in framework of acenes.[11−29] In past decades, significant advancements have been witnessed in synthesis, theoretical study, and applications of heteroacenes because heteroacenes could provide the possibility of producing cheaper and more stable electronic devices.[11−29] As one member of organic electronic devices, organic memory devices play an important role in digital logic circuits.[30−32] The data storage of organic memory devices is based on a reversible switching in low and high conduction state of organic active layer, where both states should be stable enough to maintain its information to meet the requirement for the nonvolatile memory.[30−32] Unfortunately, directly using larger oligoacenes as single active layers is impractical because most of them are not stable in low resistance state. On the other hand, heteroacenes with two different types of heteroatoms are more interesting because (1) synthesis should be more challenge, (2) more novel properties could be achieved through carefully selecting the heteroatoms in backbone and tuning their positions, and (3) heteroacenes could be more stable compared with their parent compounds. To the best of our knowledge, using heteroacenes as active layers for memory devices is unprecedented. This gap in knowledge strongly encourages us to explore the possibility.

Herein, we present two novel heteroacenes 2,3,9,10-tetra(furan-2-yl)-1,4,8,11-tetraaza-6,13-dioxapentacene (**FAOP**, **1**) and 2,3,9,10-tetra(thiophen-2-yl)-1,4,8,11-tetraaza-6,13-dioxapentacene (**TAOP**, **2**), which contain two different types of heteroatoms: O and N.

2. RESULTS AND DISCUSSION

2.1. Synthesis. **FAOP** (**1**) and **TAOP** (**2**) have been synthesized through the condensation reaction between 2,3,7,8-tetraaminodibenzo-1,4-dioxin tetrahydrochloride (**3**) and the corresponding commercially available diketones: 2,2′-furil and 2,2′-thenil (Scheme 1).[33] The important intermediate 2,3,7,8-tetraaminodibenzo-1,4-dioxin tetrahydrochloride (**3**) was synthesized in three steps according to the reported procedure.[34−36] After washing with several organic solvents, **FAOP** (**1**) and **TAOP** (**2**) were obtained as dark-yellow solids. Both compounds have a poor solubility and only slightly dissolve in polar organic solvents such as dimethylformamide (DMF) and dimethyl sulfoxide (DMSO). **FAOP** (**1**) and **TAOP** (**2**) have been fully characterized by ^{1}H NMR, ^{13}C NMR, FT-IR, and high-resolution mass spectrometry (see the Supporting Information). The thermal stability of **FAOP** (**1**) and **TAOP** (**2**) was investigated by thermal gravimetric analysis (TGA) (see Figures S5 and S6 in the Supporting Information). The

Received: May 16, 2013
Accepted: July 8, 2013
Published: July 8, 2013

Scheme 1. Synthetic Routes of FAOP, 1 and TAOP, 2[a]

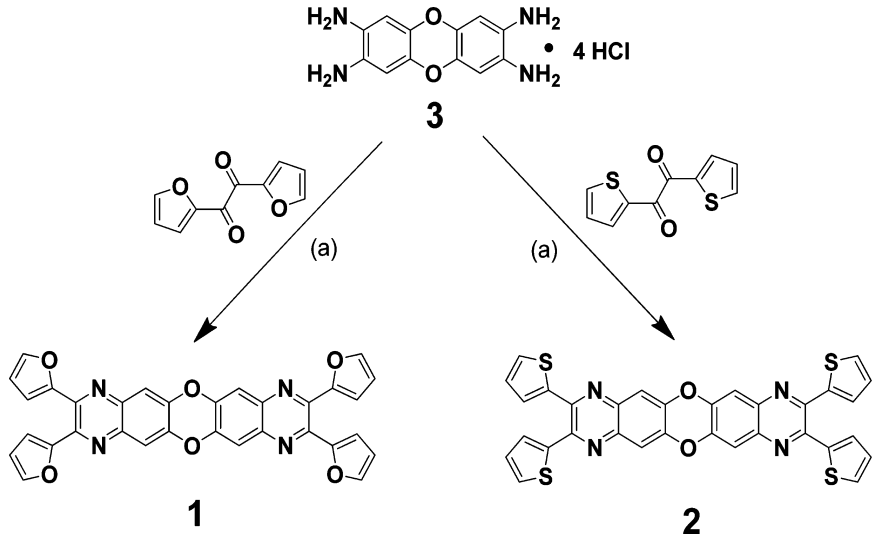

[a]Reaction conditions: (a) Acetic acid, IBX, reflux, 48 h.

curves measured under nitrogen illustrated the remarkable stability of decomposition temperature exceeded 350 °C.

2.2. Photophysical and Electrochemical Properties. The ultraviolet−visible (UV−vis) absorption spectra of **FAOP** (**1**) and **TAOP** (**2**) in dilute DMF (5×10^{-5} M) solution are shown in Figure 1A. Both the compounds exhibit two distinct absorption bands: 270−300 nm and 360−430 nm. The absorption band in the high-energy region (270−300 nm) corresponds to the $\pi-\pi^*$ electron transition of molecular backbone, whereas the one in the low-energy region (360−430 nm) can be assigned to the intramolecular charge transfer (ICT) transition. The optical bandgap for **FAOP** (**1**) and **TAOP** (**2**) is ∼2.6 eV, which is much bigger than that of their analogues: tetra(2-thioyl)-1,4,6,8,11,13-hexazapentacene (**TTHAP**, 2.25 eV).[17] This result suggests that oxygen atoms will disrupt the conjugation of **FAOP** (**1**) and **TAOP** (**2**). As observed in the previous report,[37] trifluoroacetic acid (TFA) could dramatically shift the UV−vis absorption of **FAOP** (**1**) and **TAOP** (**2**) to 540 and 535 nm, respectively, because of the protonation of N atoms in tetraazadioxapentacene backbones.

To get more insights into the electrochemical properties of **FAOP** (**1**) and **TAOP** (**2**), cyclic voltammetry (CV) measurements were carried out in dry DMF (with 0.1 M $(n\text{-}Bu)_4NPF_6$) using Ag/AgCl as a reference electrode (Figure 1B). The two fused compounds show very similar redox behaviors with one reversible reduction couple in the negative region. The onset reduction potentials for the two compounds are −1.93 V and −1.89 V, which correspond to the lowest unoccupied molecular orbital (LUMO) energy levels of about −2.47 and −2.51 eV using the equation of $E_{LUMO} = -e\,(4.40 + E_{red}^{onset})$ eV.[38] The onset oxidation potentials for **FAOP** (**1**) and **TAOP** (**2**) are 0.68 and 0.64 V, respectively, which belong to the highest occupied molecular orbital (HOMO) energy levels of −5.08 and −5.04 eV. The calculated bandgap using CV data was 2.61 and 2.53 eV for **FAOP** (**1**) and **TAOP** (**2**), which was very similar to optical onset-edge bandgap results (2.67 and 2.63 eV).

2.3. Nonvolatile Memory Behaviors. Simple resistive random-access memory (RRAM) devices were fabricated by adopting the metal−insulator−metal (MIM) structure (Figure 2). Typically, the commercially available Indium Tin Oxide

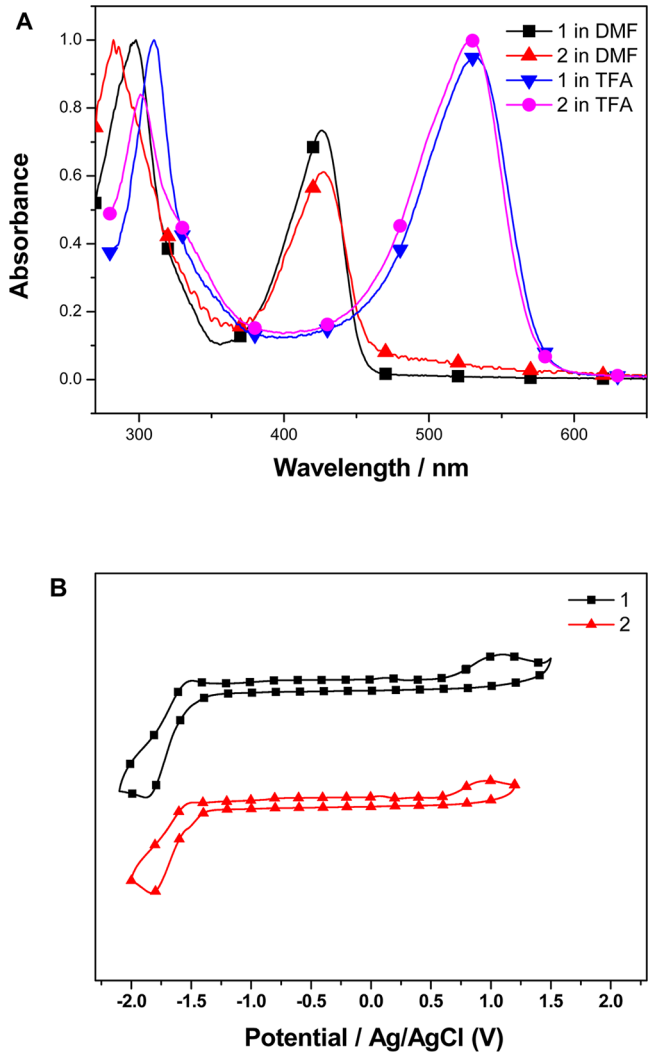

Figure 1. (A) UV−vis spectra of **FAOP** (**1**) and **TAOP** (**2**) in DMF and TFA solutions (5 × 10−5 M) and (B) cyclic voltammograms of **FAOP** (**1**) and **TAOP** (**2**) in DMF solutions at a scan rate of 50 mV/s.

dx.doi.org/10.1021/am4023434 | ACS Appl. Mater. Interfaces 2013, 5, 6458−6462

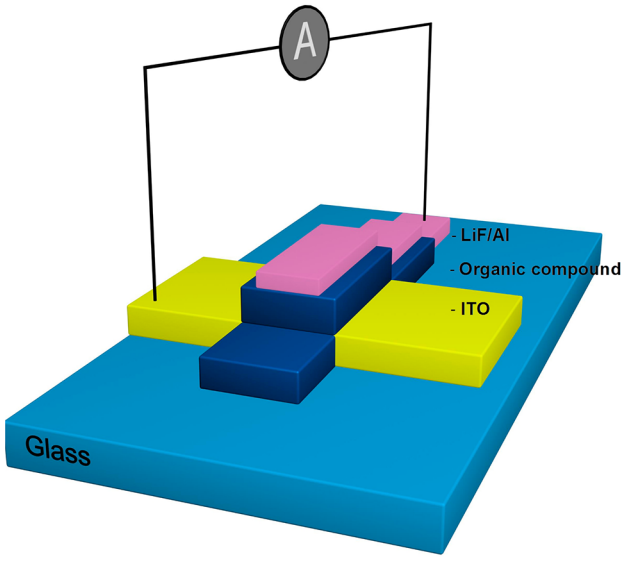

Figure 2. Scheme of the bipolar resistive switching operation devices using as-synthesized organic compounds.

(ITO) glass was employed as substrate and bottom electrode, following by depositing **FAOP** (**1**) or **TAOP** (**2**) (thickness: 50 nm) on the ITO layer by thermal evaporator. Then, a layer of 1 nm Lithium Fluoride (LiF) was evaporated on organic layer as a butter layer to decrease the possible interface barrier before depositing 150 nm Alumnum (Al) as top electrode. The current−voltage (I−V) characteristic was measured by a semiconductor parameter analyzer in diode I−V sweeping mode at room temperature. During the test, the ITO was always grounded, whereas different biases were applied on the Al top electrode.

The typical bipolar resistive switching (RS) behaviors of **FAOP** (**1**) and **TAOP** (**2**) are shown in Figure 3. The as-

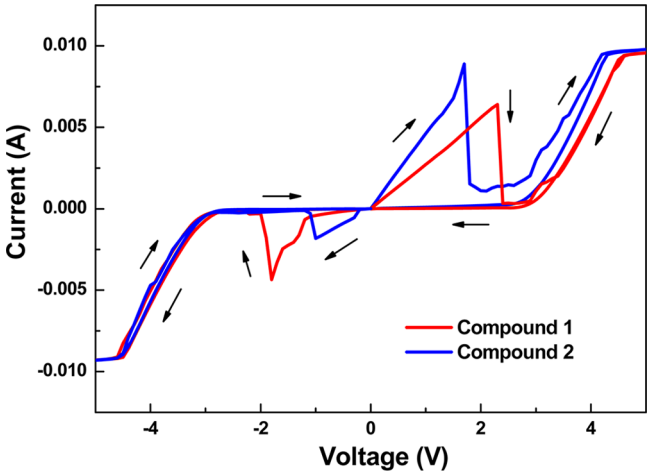

Figure 3. Bipolar resistive switching (RS) behavior of both compounds.

prepared device exhibits high resistance state (HRS), and a forming step by applying either positive or negative bias was needed to set the device to low resistance state (LRS) and trigger the RS.[39] After the forming, the devices remain LRS during the low positive voltage region when applying a small reading voltage. Until the bias reaches certain threshold value around 2−3 V, the current abruptly decreases and the devices were reset to HRS. Continuing increasing the voltage will lead to another gradual increasing of current beyond 3 V, but the devices still exhibit HRS under lower electric field when the bias sweep back to zero. Therefore, both the LRS and HRS are nonvolatile as long as the intensity of reading signal is within a small range of below 1 V. To set the device to LRS again, we required a negative bias. Similar to the phenomenon in positive region, the devices display LRS in the negative region before the bias sweeps to the corresponding threshold voltage and resets them to HRS. Repeating such an operation will start more RS cycles. To the best of our knowledge, during the past decades, many efforts have been devoted to conjugated polymer RS behavior study;[40−42] small molecular semiconductor research in this respect was rare and the two dioxapentacene derivatives demonstrating bipolar resistive switching properties was first reported in a small organic heteroacene molecule.

It is worth mentioning that at higher voltage region, the nonlinear I−V curve was observed, whereas the RS behavior only exists in the lower voltage region. Because of the near symmetric nonlinear curve, the conducting mechanism under higher electric field may attribute to the property of interior compound rather than the interface with the top and bottom electrodes. After fitting the switching curve and calculation, shown in Figure S11 in the Supporting Information, the slope is larger than 2, which denies the SCLC mode in our device. The symmetric switching curve also excludes the existence of Schottky barrier and Schottky emission in such case, hence the Poole−Frenkel (PF) emission was considered to dominate the conducting at higher voltage region (the direct evidence of plot of $\log(I/V)$ versus $\mathrm{sqrt}(V)$ at HRS is shown in Figure S12 in the Supporting Information), mainly originating from electric-field-enhanced thermal excitation of electrons in defect-related trapped states.[43] As for the RS behavior in lower voltage region, it is usually explained by a filamentary conducting path formed in the functional material (see illustration S9 in the Supporting Information).[44] By the forming step, a conductive filament was produced and lead to the near Ohmic conducting behavior in LRS. However, the filament would be dissolved when increasing the voltage due to the Joule Heating effect under high current.[45] Joule heating is unwanted but inevitable side effect caused in RS operation, and probably accounts for the unsatisfactory endurance performance of our devices. After around ten cycles, we failed to observe RS behavior and the devices display only nonlinear conduction as shown in the high-voltage region.

The write-read-erase-read operation of our organic RRAM device based on **FAOP** (**1**) is demonstrated in Figure 4 (the endurance and retention property of the device are shown in Figures S13 and S14 in the Supporting Information). A positive pulse of 1 V was applied as a reading signal, whereas the pulses of 3 V and −3 V were employed as erasing and writing signals, respectively. The corresponding resistance of each reading cycle was shown below the pulse series. The on/off ratio of our device is around 1×10^2, although there exists small fluctuation of resistance distribution in both HRS and LRS. Because of the symmetric bipolar switching characteristic of the device, similar operation could also be realized in the opposite voltage region with −1 V/−3 V/−1 V/3 V/−1 V pulse series, where the −3 V is erasing signal and 3 V is writing signal.

dx.doi.org/10.1021/am4023434 | ACS Appl. Mater. Interfaces 2013, 5, 6458−6462

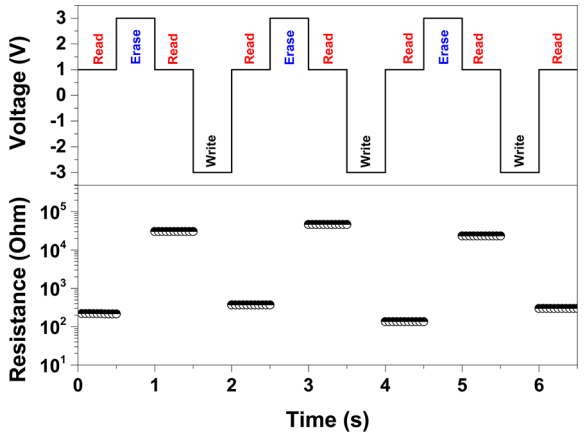

Figure 4. Write-read-erase-read operation of as-fabricated organic RRAM device based on **FAOP** (**1**).

3. EXPERIMENTAL SECTION

3.1. General Remarks. 2,2′-furil and 2,2′-thenil were purchased from Aldrich company. 2,3,7,8-Tetraaminodibenzo-1,4-dioxin tetrahydrochloride was synthesized according to a reported procedure.[35] Other chemicals and solvents were used directly without further purification. Solution NMR spectra were taken on a Bruker Advance 400 spectrometer. Electrochemistry was carried out with a CHI 600C potentiostat, employing glassy carbon (diameter: 1.6 mm; area 0.02 cm^2), a platinum wire, and silver/silver chloride (Ag/AgCl) as working, counter, and reference electrode, respectively. Tetrabutylammonium Hexafluorophosphate (0.1M) dissolved in dry dimethylformamide (DMF) solution was used as an electrolyte at room temperature under the protection of argon. The potential was externally calibrated against the ferrocene/ferrocenium couple. HR-MS (ESI) spectra were recorded on a Waters Q-Tof premierTM mass spectrometer. UV−vis spectrum was recorded using a Shimadzu UV-2501 spectrometer. Thermogravimetric analysis (TGA) was carried out on a TA Instrument Q500 thermogravimetric analyzer at a heating rate of 10 °C/min up to 700 °C.

3.2. Nonvolatile Memory Device Fabrication. Typically, the commercially available ITO glass with pattern in advance was employed as substrate and bottom electrode, and all the other films were deposited by using the same evaporator at room temperature. The FAOP (1) or TAOP (2) powder placed in a small crucible were evaporated on to the ITO substrate with thickness controlled at around 50 nm. Then, a layer of 1 nm LiF was evaporated on the organic layer as a butter layer to decrease the possible interface barrier before depositing 150 nm Al as top electrode.

3.3. Synthesis. *2,3,9,10-Tetra(2-furanyl)-1,4,8,11-tetraaza-6,13-dioxapentacene* ***FAOP (1).*** 2,3,7,8-tetraaminodibenzo-1,4-dioxin tetrahydrochloride (180 mg, 0.46 mmol), furil (209 mg, 1.1 mmol) and 2-iodoxybenzoic acid (IBX, 5 mg) were dissolved into anhydrous acetic acid (20 mL) . The solution was refluxed for 48 h. After cooling to room temperature, the precipitate was filtered and washed with chloroform, ethanol, acetone, and tetrahydrofuran and yielded **FAOP** (**1**) (145 mg,57%) as a dark-yellow solid. ^{1}H NMR (400 MHz, TFA-*d*, *δ*): 8.02 (s, 4H, Ar H), 7.88 (s, 4H, Ar H), 7.26 (d, 4H, Ar H), 6.82 (s, 4H, Ar H). ^{13}C NMR (100 MHz, TFA-*d*, *δ*): 148.99, 145.60, 144.27, 138.49, 133.37, 121.45, 114.01, 110.25. FT-IR (KBr, cm^{-1})): 1473(C═N). HRMS (ESI): (M + H) $^+$ calcd for $C_{32}H_{17}N_4O_6$, 553.1148; found 553.1112.

2,3,9,10-Tetra(2-thioyl)-1,4,8,11-tetraaza-6,13-dioxapentacene ***(TAOP, 2).*** 2,3,7,8-Tetraaminodibenzo-1,4-dioxin tetrahydrochloride (180 mg, 0.46 mmol), 2,2′-thenil (244 mg, 1.1 mmol) and IBX (5 mg) were dissolved into anhydrous acetic acid (20 mL). The solution was refluxed for 48 h. After being cooled to room temperature, the precipitate was filtered and washed with dichloromethane, ethanol, and acetone to yield **TAOP** (**2**) (140 mg, 49%) as a dark- yellow solid. ^{1}H NMR (400 MHz, TFA-*d*, *δ*): 8.01 (s, 4H, Ar H), 7.85 (d, 4H, Ar H), 7.65 (d, 4H, Ar H), 7.24 (t, 4H, Ar H). ^{13}C NMR (100 MHz, TFA-*d*, *δ*): 145.87, 145.68, 134.57, 134.38, 133.96, 131.96, 128.46, 110.13. FT-IR (KBr, cm^{-1})): 1473(C═N). HRMS (ESI): (M + H) $^+$ calcd for $C_{32}H_{17}N_4O_2S_4$, 617.0234; found 617.0290.

4. CONCLUSIONS

In summary, we have successfully synthesized two novel heteroacenes containing two different types of heteroactoms (N, O) in their backbones. The sandwich-structure memory devices using **FAOP** (**1**) and **TAOP** (**2**) as active layers have been fabricated. Both compounds show a typical bipolar resistive switching (RS) behavior in positive and negative regions. We hope that our results will provide guidance for the design and synthesis of new heteroacenes, which could be used as promising candidates in nonvolatile memory devices.

■ ASSOCIATED CONTENT

Supporting Information

^{1}H NMR, ^{13}CNMR, FT-IR profile, TGA profile, and high-solution mass spectrum (HRMS) profile. This material is available free of charge via the Internet at http://pubs.acs.org.

■ AUTHOR INFORMATION

Corresponding Author

*E-mail: qczhang@ntu.edu.sg (Q.Z.); xwsun@sustc.edu.cn (X.W.S.); fzhu@nankai.edu.cn (F.H.).

Notes

The authors declare no competing financial interest.

■ ACKNOWLEDGMENTS

Q.Z. acknowledges the financial support from AcRF Tier 1 (RG 16/12) from MOE, MOE Tier 2, CREATE program (Nanomaterials for Energy and Water Management) from NRF, and New Initiative Fund from NTU, Singapore. F.H. thanks the financial support from the Natural Science Foundation (11JCYBJC14200) of Tianjin City, China.

■ REFERENCES

(1) Watanable, M.; Chang, Y. J.; Liu, S.-W.; Chao, T.-H.; Goto, K.; Yuan, Md. M. I. C.-H.; Tao, Y.-T.; Shinmyozu, T.; Chow, T. J. *Nat. Chem.* **2012**, *4*, 574−578.

(2) Xiao, J.; Duong, H. M.; Liu, Y.; Shi, W.; Ji, L.; Li, G.; Li, S.; Liu, X.; Ma, J.; Wudl, F.; Zhang, Q. *Angew Chem., Int. Ed.* **2012**, *51*, 6094−6098.

(3) Xiao, J.; Malliakas, C. D.; Liu, Y.; Zhou, F.; Li, G.; Su, H.; Kanatzidis, M. G.; Wudl, F.; Zhang, Q. *Chem. Asian J.* **2012**, *4*, 672−675.

(4) Purushothaman, B.; Bruzek, M.; Parkin, S. R.; Miller, A.-F.; Anthony, J. E. *Angew Chem., Int. Ed.* **2011**, *50*, 7013−7017.

(5) Kaur, I.; Jazdzky, M.; Stein, N. N.; Prusevich, P.; Miller, G. P. *J. Am. Chem. Soc.* **2010**, *132*, 1261−1263.

(6) Anthony, J. E. *Angew. Chem., Int. Ed.* **2008**, *47*, 452−483.

(7) Anthony, J. E. *Chem. Rev.* **2006**, *106*, 5028−5048.

(8) Xiao, J.; Liu, S.; Liu, Y.; Ji, L.; Liu, X.; Zhang, H.; Sun, X.; Zhang, Q. *Chem. Asian J.* **2012**, *7*, 561−564.

(9) Xiao, J.; Divayana, Y.; Zhang, Q.; Duong, H. M.; Zhang, H.; Boey, F.; Sun, X. W.; Wudl, F. *J. Mater. Chem.* **2010**, *20*, 8167−8170.

(10) Zhang, Q.; Divayana, Y.; Xiao, J.; Wang, Z.; Tiekink, E. R. T.; Duong, H. M.; Zhang, H.; Boey, F.; Sun, X. W.; Wudl, F. *Chem.—Eur. J.* **2010**, *16*, 7422−7426.

(11) He, Z.; Mao, R.; Liu, D.; Miao, Q. *Org. Lett.* **2012**, *14*, 4190−4193.

(12) He, Z.; Liu, D.; Mao, R.; Tang, Q.; Miao, Q. *Org. Lett.* **2012**, *14*, 1050−1053.

(13) Liang, Z.; Tang, Q.; Xu, J.; Miao, Q. *Adv. Mater.* **2011**, *23*, 1535−1539.
(14) Lindner, B. D.; Engelhart, J. U.; Märken, M.; Tverskoy, O.; Appleton, A. L.; Rominger, F.; Hardcastle, K. I.; Enders, M.; Bunz, U. H. F. *Chem.—Eur. J.* **2012**, *18*, 4627−4633.
(15) Lindner, B. D.; Engelhart, J. U.; Tverskoy, O.; Appleton, A. L.; Rominger, F.; Peters, A.; Himmel, H.-J.; Bunz, U. H. F. *Angew Chem., Int. Ed.* **2011**, *50*, 8588−8591.
(16) Appleton, A. L.; Brombosz, S. M.; Barlow, S.; Sears, J. S.; Bredas, J.-L.; Marder, S. R.; Bunz, U. H. F. *Nat. Commun.* **2010**, *1*, 91−96.
(17) Li, G.; Wu, Y.; Gao, J.; Wang, C.; Li, J.; Zhang, H.; Zhao, Y.; Zhao, Y.; Zhang, Q. *J. Am. Chem. Soc.* **2012**, *134*, 20298−2030.
(18) Li, G.; Putu, A. A.; Gao, J.; Divayana, Y.; Chen, W.; Zhao, Y.; Sun, X. W.; Zhang, Q. *Asian J. Org. Chem.* **2012**, *1*, 346−351.
(19) Li, G.; Duong, H. M.; Zhang, Z.; Xiao, J.; Liu, L.; Zhao, Y.; Zhang, H.; Hua, F.; Li, S.; Ma, J.; Wudl, F.; Zhang, Q. *Chem. Comm* **2012**, *48*, 5974−5976.
(20) Wu, Y.; Yin, Z.; Xiao, J.; Liu, Y.; Wei, F.; Tan, K. J.; Kloc, C.; Huang, L.; Yan, Q.; Hu, F.; Zhang, H.; Zhang, Q. *ACS Appl. Mater. Interfaces* **2012**, *4*, 1883−1886.
(21) Zhang, Q.; Xiao, J.; Yin, Z.; Duong, H. M.; Qiao, F.; Boey, F.; Hu, X.; Zhang, H.; Wudl, F. *Chem. Asian. J.* **2011**, *6*, 856−862.
(22) Winkler, M.; Houk, K. N. *J. Am. Chem. Soc.* **2007**, *129*, 1805−1815.
(23) Gao, B.; Wang, M.; Cheng, Y.; Wang, L.; Jing, X.; Wang, F. *J. Am. Chem. Soc.* **2008**, *130*, 8297−8306.
(24) Liu, Y.-Y.; Song, C.-L.; Zeng, W.-J.; Zhou, K.-G.; Shi, Z.-F.; Ma, C.-B.; Yang, F.; Zhang, H.-L.; Gong, X. *J. Am. Chem. Soc.* **2010**, *132*, 16349−16351.
(25) Tong, C.; Zhao, W.; Luo, J.; Mao, H.; Chen, W.; Chan, H. S. O.; Chi, C. *Org. Lett.* **2012**, *14*, 494−497.
(26) Li, J.; Zhang, Q. *Synlett* **2013**, *24*, 686−696.
(27) Zhao, J.; Wong, J. I.; Wang, C.; Gao, J.; Ng, V. Z. Y; Yang, H. Y.; Loo, C. J.; Zhang, Q. *Chem. Asian J.* **2013**, *8*, 665−669.
(28) Wang, C.; Li, G.; Zhang, Q. *Tetrahedron Lett.* **2013**, *54*, 2633−2636.
(29) Zhao, J.; Li, G.; Wang, C.; Chen, W.; Loo, S. C. J.; Zhang, Q. *RSC Adv.* **2013**, *3*, 9653−9657.
(30) Li, H.; Xu, Q.; Li, N.; Sun, R.; Ge, J.; Lu, J.; Gu, H.; Yan, F. *J. Am. Chem. Soc.* **2010**, *132*, 5542−5543.
(31) Miao, S.; Li, H.; Xu, Q.; Li, Y.; Ji, S.; Li, N.; Wang, L.; Zheng, J.; Lu, J. *Adv. Mater.* **2012**, *24*, 6210−6215.
(32) Ye, C.; Peng, Q.; Li, M.; Luo, J.; Tang, Z.; Pei, J.; Chen, J.; Shuai, Z.; Jiang, L.; Song, Y. *J. Am. Chem. Soc.* **2012**, *134*, 20053−20059.
(33) Li, G.; Long, G.; Chen, W.; Hu, F.; Chen, Y.; Zhang, Q. *Asian J. Org. Chem.* **2013**, DOI: 10.1002/ajoc.201300095.
(34) Denysenko, D.; Grzywa, M.; Tonigold, M.; Streppel, B.; Krkljus, I.; Hirscher, M.; Mugnaioli, E.; Kolb, U.; Hanss, J.; Volkmer, D. *Chem.—Eur. J.* **2011**, *17*, 1837−1848.
(35) Chichak, K.; Jacquemard, U.; Branda, N. R. *Eur. J. Inorg. Chem.* **2002**, 357−368.
(36) Gilman, H.; Dietrich, J. J. *J. Am. Chem. Soc.* **1958**, *80*, 366−368.
(37) Zucchero, A. J.; McGrier, P. L.; Bunz, U. H. F. *Acc. Chem. Res.* **2010**, *43*, 397−408.
(38) Zhang, W.; Sun, X.; Xia, P.; Huang, J.; Yu, G.; Wong, M. S; Yunqi Liu, Y.; Zhu, D. *Org. Lett.* **2012**, *14*, 4382−4385.
(39) Waser, R.; Aono, M. *Nat. Mater.* **2007**, *6*, 833−840.
(40) Lian, S.-L.; Liu, C.-L.; Chen, W.-C. *ACS Appl. Mater. Interfaces* **2011**, *3*, 4504−4511.
(41) Cho, B.; Song, S.; Ji, Y.; Kim, T.-W.; Lee, T. *Adv. Funct. Mater.* **2011**, *21*, 2806−2829.
(42) Yang, Y.; Ouyang, J.; Ma, L.; Tseng, R. J. H.; Chu, C. W. *Adv. Funct. Mater.* **2006**, *16*, 1001−1014.
(43) Choi, J. S.; Kim, J. S.; Hwang, I. R.; Jeon, S. H.; Kang, S. O.; Park, B. H.; Kim, D. C.; Lee, M. J.; Seo, S. *Appl. Phys. Lett.* **2009**, *95*, 022109.
(44) Yang, Y. C.; Pan, F.; Liu, Q. *Nano Lett.* **2009**, *9*, 1636−1643.
(45) Scott, J. C.; Bozano, L. D. *Adv. Mater.* **2007**, *19*, 1452−1463.